ACS chemical biology

Articles

pubs.acs.org/acschemicalbiology

Terms of Use

Cupric Yersiniabactin Is a Virulence-Associated Superoxide Dismutase Mimic

Kaveri S. Chaturvedi,[†,‡,§] Chia S. Hung,[†,‡,§] Daryl E. Giblin,[∥] Saki Urushidani,[‡] Anthony M. Austin,[⊥] Mary C. Dinauer,[⊥,#] and Jeffrey P. Henderson*[,†,‡,§]

[†]Center for Women's Infectious Diseases Research, [‡]Division of Infectious Diseases, [§]Department of Internal Medicine, [∥]Department of Chemistry, [⊥]Department of Pediatrics, and [#]Department of Pathology and Immunology, Washington University School of Medicine, St. Louis, Missouri 63110, United States

Supporting Information

ABSTRACT: Many Gram-negative bacteria interact with extracellular metal ions by expressing one or more siderophore types. Among these, the virulence-associated siderophore yersiniabactin (Ybt) is an avid copper chelator, forming stable cupric (Cu(II)-Ybt) complexes that are detectable in infected patients. Here we show that Ybt-expressing *E. coli* are protected from intracellular killing within copper-replete phagocytic cells. This survival advantage is highly dependent upon the phagocyte respiratory burst, during which superoxide is generated by the NADPH oxidase complex. Chemical fractionation links this phenotype to a previously unappreciated superoxide dismutase (SOD)-like activity of Cu(II)-Ybt. Unlike previously described synthetic copper-salicylate (Cu(II)-SA) SOD mimics, the salicylate-based natural product Cu(II)-Ybt retains catalytic activity at physiologically plausible protein concentrations. These results reveal a new virulence-associated adaptation based upon spontaneous assembly of a non-protein catalyst.

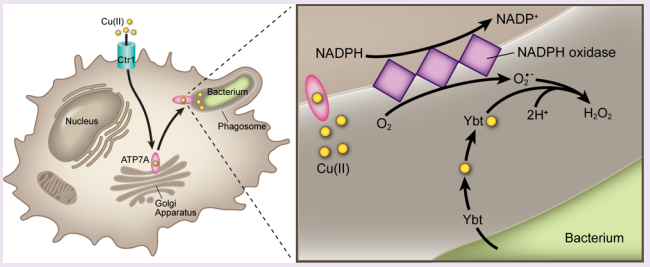

Pathogenic Gram-negative bacteria secrete chemically diverse low molecular weight virulence factors called siderophores. These small molecules solubilize host ferric iron for import as a bacterial nutrient source and transport it back to the bacteria by means of high affinity transporters (see review, ref 1). The virulence of pathogenic *Enterobacteriaceae*, including highly virulent strains of *Yersinia pestis* (agent of the black plague) and uropathogenic *Escherichia coli* (UPEC) is strongly linked to expression of the salicylate-based siderophore yersiniabactin (Ybt).[2−6] Ybt's biosynthetic (*ybtT*, *ybtE* ,*ybtS*), transport (*fyuA*, *ybtP*, *ybtQ*), and regulatory (*ybtA*) genes are encoded by a chromosomal locus designated the *Yersinia* high-pathogenicity island (HPI).[7] Ybt's iron scavenging activity conforms to the canonical Gram-negative siderophore process in which it binds ferric iron, is actively transported through the outer membrane *via* a TonB-dependent β barrel protein (FyuA), and subsequently delivers iron to the cytosol through ATP cassette proteins (YbtPQ). Recently, we have shown that Ybt can protect bacteria from metal toxicity independently of transporter proteins by sequestering cupric ions (Cu(II)) as stable extracellular complexes (Cu(II)-Ybt) in patients infected with uropathogenic *Escherichia coli* (UPEC).[8]

Physiologic studies have demonstrated that infection is accompanied by systemic changes in copper concentration within the host (see review, ref 9). The plasma concentration of ceruloplasmin, the primary host copper-transporting protein, increases during inflammation or infection, leading to copper accumulation at sites of inflammation.[10−12] Elemental analysis and radiotracer studies have shown concentrations of copper up to several hundred micromolar within granulomatous lesions in lungs infected by *Mycobacterium tuberculosis* and at sites of inflammation such as wound exudates and burns where macrophages congregate.[13−16] Genes encoding mammalian copper uptake are upregulated in macrophages infected by *Mycobacterium tuberculosis*, *Salmonella typhimurium*, and other intracellular pathogens.[17−20] Phagocytes such as macrophages represent one of the first lines of defense against invading microbial pathogens and rely on high local concentrations for copper(II) for their bactericidal action.[21,22] Impairment of copper transport to the macrophage phagosome disrupts normal immune function in these cells and permits increased bacterial survival following phagocytosis.

In this study we used cellular, chemical, and computational approaches to evaluate the hypothesis that Ybt's previously documented copper-binding activity protects UPEC during phagocytosis. Our results indicate that Ybt expression confers a copper-dependent intracellular survival advantage in multiple phagocytic cell types. This survival advantage is minimized in phagocytes with pharmacologic or genetic deficiencies in NADPH oxidase-derived superoxide production. The chemical basis for these findings is a SOD-like activity attributed to Cu(II)-Ybt complexes. Together, these studies provide new

Received: August 30, 2013
Accepted: November 27, 2013
Published: November 27, 2013

 © 2013 American Chemical Society dx.doi.org/10.1021/cb400658k | *ACS Chem. Biol.* 2014, 9, 551−561

insights into how pathogenic bacteria use secondary metabolites to survive innate host defenses.

RESULTS AND DISCUSSION

Ybt Promotes *E. coli* Survival in RAW264.7 Cells. To determine whether Ybt expression protects phagocytosed bacteria from the copper-dependent bactericidal activity of macrophage-like RAW264.7 cells, we compared intracellular survival of the model uropathogen UTI89 to its isogenic Ybt-deficient mutant UTI89Δ*ybtS* (Figure 1a). As described in the copper-dependent *E. coli* bactericidal system by White *et al.*,[22] we infected RAW264.7 cells with or without overnight preincubation in copper-containing media with UTI89 or UTI89Δ*ybtS* at a multiplicity of infection (MOI, ratio of bacteria to mammalian cells) of 10. Following gentamycin treatment to ensure assessment of intracellular bacteria only, viable bacteria were determined 1 h after infection by colony forming unit (CFU/mL) determination. The number of internalized bacteria were unaffected by either RAW264.7 cell copper availability or bacterial strain. In copper-replete RAW264.7 cells, wild type UTI89 exhibits significantly greater (~2 log CFU/mL, $p = 0.001$) survival than UTI89Δ*ybtS*. The survival difference between wild type UTI89 and UTI89Δ*ybtS* survival is eliminated in copper-deficient RAW264.7 cells. These results show that Ybt expression promotes UPEC intracellular survival in copper-replete RAW264.7 cells.

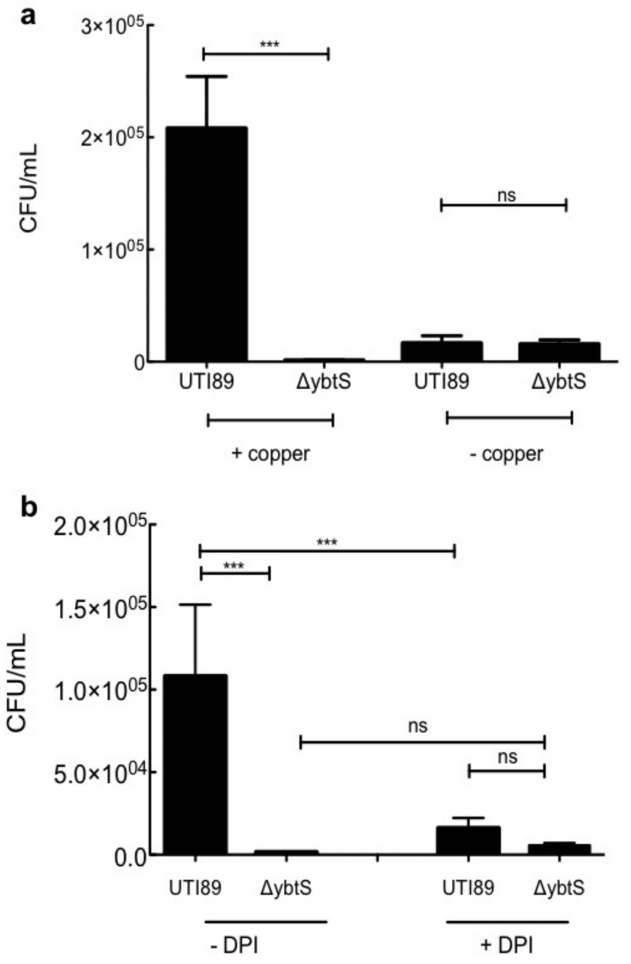

Figure 1. Yersiniabactin promotes intracellular uropathogen survival in a copper- and respiratory burst-dependent manner. RAW264.7 macrophage-like cells were infected with the uropathogen UTI89 and its yersiniabactin-deficient UII89ΔybtS mutant. Intracellular bacterial survival after 1 h was expressed as a difference from initial internalized *E. coli* in three separate experiments. (a) In RAW264.7 cells cultured in the presence of 20 μM copper sulfate, intracellular UTI89 survival was significantly higher than that of UTI89ΔybtS (mean ± SD; $n = 3$; $p = 0.0032$, *t* test). This survival advantage was minimized in RAW264.7 cells that were not preincubated with copper. (b) Addition of 20 μM NADPH oxidase inhibitor diphenyleneiodonium chloride (DPI) to RAW264.7 macrophages cultured with copper sulfate diminished UTI89's survival advantage over UTI89ΔybtS (12-fold survival advantage, $p = 0.0044$, *t* test).

Ybt may benefit intracellular pathogens by sequestering copper outside the bacterial cell or mediating metal ion import through the outer membrane ferric-yersiniabactin importer FyuA. To distinguish between these possibilities, we compared the intracellular survival of isogenic FyuA-deficient strains with and without Ybt biosynthetic activity (UTI89Δ*fyuA* and UTI89Δ*fyuA*Δ*ybtS*, respectively, Supplemental Figure S1). Even in the absence of FyuA, the Ybt-expressing strain (UTI89Δ*fyuA*) still displayed a significant intracellular survival advantage (approximately 1.77 log CFU/mL, $p = 0.001$) in copper-replete RAW264.7 cells compared to the double mutant. This survival advantage was eliminated in copper-deficient RAW264.7 cells. Ybt's protective effect in copper-replete RAW264.7 cells thus persists even when its value as a ferric ion siderophore is negated by a null mutation of the Ybt importer. These observations show that Ybt expression can promote UPEC intracellular survival independently of its cognate outer membrane transporter.

Ybt-Dependent Survival Is Maximal during the Respiratory Burst. UTI89 exhibited greater intracellular survival in copper-replete RAW264.7 cells ($p = 0.018$ when compared to RAW cells cultured without copper, *t* test). No such advantage was observed with non-pathogenic K12 cells in this (Supplemental Figure S2) or a prior study.[22] One possible explanation for this copper-dependent gain of function is that the Cu(II)-Ybt complexes formed within the phagolysosome of copper-replete RAW264.7 cells catalyze superoxide dismutation similarly to synthetic Cu(II)-salicylate (Cu(II)-SA) complexes.[23−25] To evaluate this hypothesis we compared wild type UTI89 and UTI89Δ*ybtS* survival in RAW 264.7 cells treated with the NADPH oxidase inhibitor diphenyleneiodonium chloride (DPI, Figure 1b). DPI treatment substantially diminished UTI89's survival advantage over UTI89Δ*ybtS* ($p = 0.0044$ when compared to DPI untreated UTI89, *t* test) and became statistically insignificant. Without copper repletion, UTI89 and UTI89Δ*ybtS* survival was indistinguishable in DPI-treated RAW 264.7 cells (Supplemental Figure S3). These findings show that Ybt's copper-dependent intracellular survival advantage is maximal in the presence of respiratory burst-derived superoxide.

UTI89 Exhibits a Competitive Survival Advantage in RAW 264.7 Cells. To more directly compare intracellular survival of Ybt-expressing and non-expressing bacteria, RAW 264.7 cells were co-infected with a 1:1 mixture of wild type UTI89::kan and UTI89Δ*ybtS*. Ybt-specific intracellular fitness was determined by comparing each strain's relative intracellular survival (calculated as log competitive survival indices; see Methods). In copper-replete RAW264.7 cells, Ybt-expressing UTI89 exhibited a significant survival advantage over UTI89Δ*ybtS* (competitive index > 0, $p = 0.0039$, Wilcoxon signed-rank test) (Figure 2a). This competitive advantage was abolished in copper-depleted RAW 264.7 cells. These results

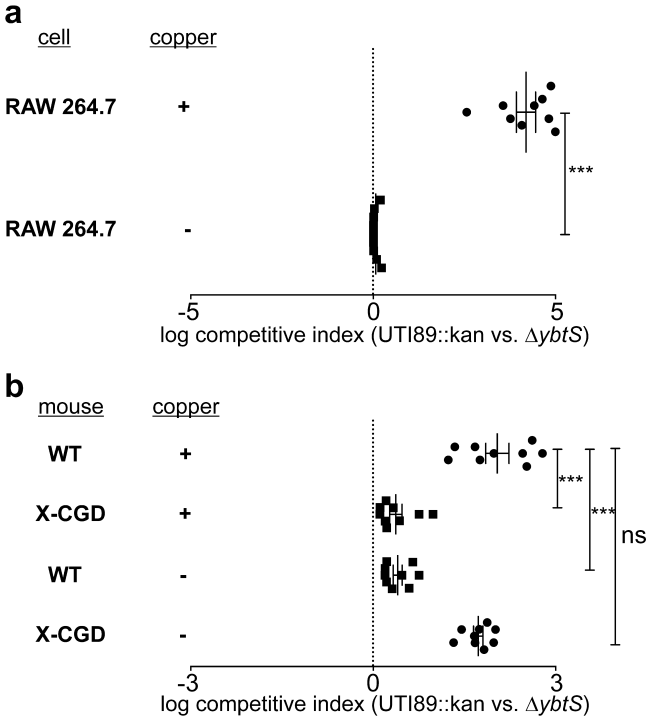

Figure 2. Ybt-expressing bacteria exhibit a copper- and superoxide-dependent competitive survival advantage within phagocytes. Competitive co-infection of wild type UTI89 and its Ybt-deficient UTI89Δ*yAtS* mutant was assessed in (a) RAW264.7 cells and (b) resident peritoneal macrophages from wild type and respiratory burst-deficient X-CGD (gp91$^{phox-/-}$) mice. A competitive index (CI) value greater than zero indicates a wild type UTI89 survival advantage, such that a log CI of 1 indicates 10-fold greater UTI89 survival. (a) A higher CI in copper-replete RAW264.7 cells indicates preferential survival of UTI89 over the Ybt biosynfhetic mutant (log CI 4.2 *vs* 0.7, $p = 0.0039$, Wilcoxon signed-rank test). (b) Log CI is higher in copper-replete wild type mouse macrophages than in copper-replete X-CGD mouse macrophages (log CI 2 *vs* 0.4, $p = 0.0041$, Wilcoxon signed-rank test). In the absence of copper, this relationship was reversed (log CI 0.4 *vs* 1.7 $p = 0.0036$, Wilcoxon signed-rank test).

show that Ybt expression selectively promotes UPEC intracellular survival in copper-replete RAW264.7 cells during identical culture conditions.

Ybt Affects Survival in Respiratory Burst-Competent Peritoneal Macrophages. To determine whether a genetic respiratory burst deficiency in macrophages impacts Ybt's survival advantage, we compared competitive intracellular survival in murine resident peritoneal macrophages derived from wild type C57BL/6 to those from X-CGD (gp91$^{phox-/-}$) mice. X-CGD (gp91$^{phox-/-}$) mice have a disruption in the gene encoding the 91 kD subunit of oxidase cytochrome *b* and therefore lack phagocyte superoxide production.[26] Competitive infection with Ybt-expressing and non-expressing UTI89 strains (UTI89::kan *vs* UTI89Δ*ybtS*) was assessed in resident peritoneal macrophages from wild type C57BL/6 and X-CGD (gp91$^{phox-/-}$) mice (Figure 2b). In copper-replete wild type peritoneal macrophages, Ybt-expressing wild type UTI89 exhibited a significant survival advantage over Δ*ybtS* (log CI 2, $p = 0.0041$, Wilcoxon signed-rank test) (Figure 2b). This competitive advantage was significantly diminished when copper was omitted in wild type C57BL/6 macrophages or when copper-replete X-CGD macrophages were used (CI of 0.4 and 0.4, $p = 0.0036$ and 0.0041, respectively, Wilcoxon signed-rank test). These findings further support a role for Cu(II)-Ybt in resisting superoxide-derived host defenses in mouse peritoneal macrophages. Without copper supplementation, an elevated CI (CI of 1.7, $p < 0.0039$, Wilcoxon signed-rank test) was noted in X-CGD macrophages, consistent with a copper-independent Ybt function that facilitates UTI89 survival in peritoneal macrophages but not RAW 264.7 cells.

To determine whether the survival differences noted in murine macrophages require Ybt import, we determined competitive indices for UTI89 and its transport-deficient Δ*fyuA* mutant (UTI89::kan *vs* Δ*fyuA*). Unlike UTI89Δ*ybtS*, UTI89Δ*fyuA* and wild type UTI89 survival were indistinguishable in all conditions ($p = 0.7712$, Wilcoxon signed-rank test), consistent with a critical role for Ybt biosynthesis, not uptake, in intracellular survival (Supplemental Figure S4). In summary, although peritoneal macrophages and RAW264.7 cells have different cellular origins and deploy different antimicrobial effectors,[27−30] Ybt-expressing *E. coli* exhibit an intracellular survival advantage in copper-replete phagocytes during the respiratory burst that is independent of the ferric-Ybt transporter FyuA.

Cu(II)-Ybt Exhibits Superoxide Dismutase-Like Activity. We hypothesized that Ybt or related products protect intracellular pathogens from the respiratory burst within copper-containing phagosomes by forming Cu(II) complexes that mimic superoxide dismutases. Cu(II)-SA complexes with this activity have been described extensively and were once proposed for pharmaceutical use.[23,31−37] To determine whether wild type UTI89 culture supernatants exhibit superoxide dismutase (SOD)-like activity in the presence of copper, minimal media culture supernatants from UTI89 and UTI89Δ*ybtS* were fractionated and screened for SOD activity (Figure 3a and b) using the xanthine/xanthine oxidase reaction WST-formazan-based superoxide assay.[38,39] Activities are expressed relative to 100 μM bovine Cu,Zn-SOD standard. Maximal SOD activity was observed in the 80% methanolic extract of copper-supplemented wild type UTI89 (87.6% of total supernatant activity). This active fraction was absent in copper-deficient or UTI89Δ*ybtS* fractions.

To determine the origin of SOD-like activity in copper-replete wild-type supernatants, we analyzed fractions by liquid chromatography−mass spectrometry (LC−MS). The LC−MS chromatogram from the 80% fraction was dominated by a single peak corresponding to Cu(II)-Ybt (Figure 3c). A preparation of purified Cu(II)-Ybt similarly exhibited SOD-like activity with a dose−response relationship (Figure.4a). For 0.12, 0.6, 3.0, and 15.0 mM solutions of Cu(II)-Ybt, the percentage inhibition rates were determined to be 4.6%, 19.8%, 24.3%, and 55.7%, respectively.

Superoxide dismutase catalyzes the dismutation of superoxide into oxygen and hydrogen peroxide (H_2O_2). This reaction classically requires a redox active metal (M) to propagate the following reactions:

$$\text{SOD-M}^{(n+1)+} + O_2^{\bullet -} \rightarrow \text{SOD-M}^{n+} + O_2 \quad (1)$$

$$\text{SOD-M}^{n+} + O_2^{\bullet -} + 2H^+ \rightarrow \text{SOD-M}^{(n+1)+} + H_2O_2 \quad (2)$$

To function as a catalyst, Cu(II)-Ybt must be regenerated, not consumed, during superoxide exposure. We therefore used LC−MS to quantify purifed Cu(II)-Ybt following exposure to the complete or incomplete xanthine/xanthine oxidase system (Figure 4b). Cu(II)-Ybt concentration was not significantly

dx.doi.org/10.1021/cb400658k | *ACS Chem. Biol.* 2014, 9, 551−561

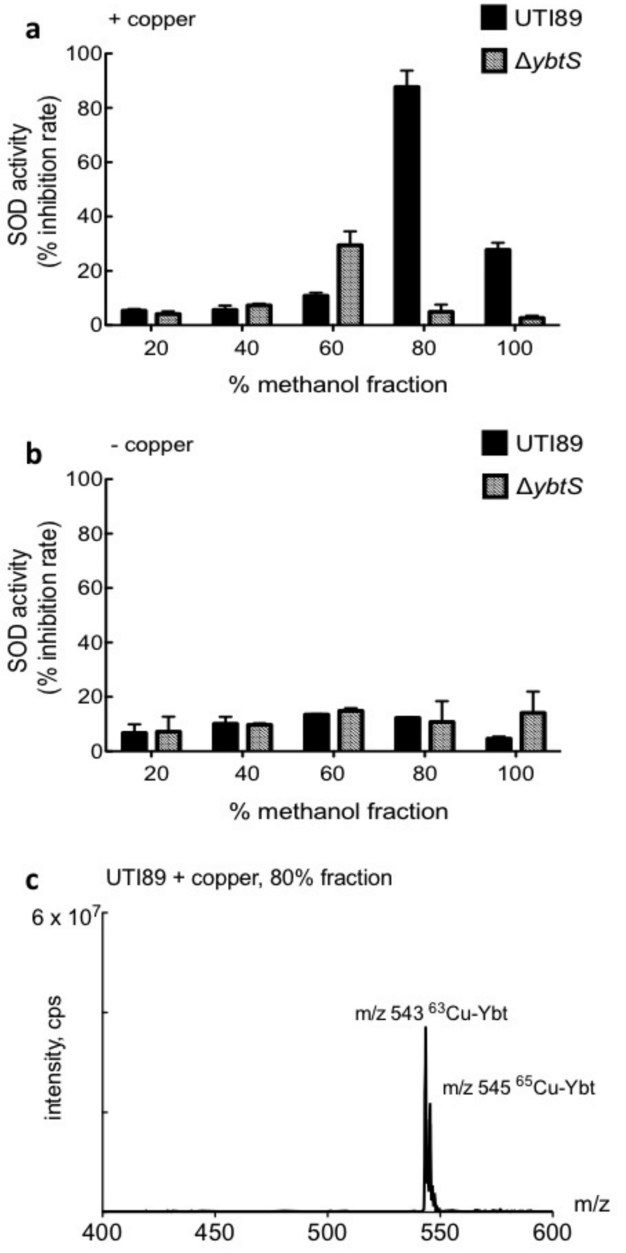

Figure 3. UTI89 supernatants exhibit superoxide dismutase activity following copper addition. Copper-treated and untreated culture supernatant fractions of UTI89 and UTI89ΔybtS were tested for superoxide dismutase (SOD) activity. SOD activity is expressed as inhibition of xanthine oxidase-generated superoxide levels relative to 100 μM Cu,Zn-SOD standard (defined as 100% inhibition). (a) SOD activity is observed in the 80% methanolic extracts of copper-replete UTI89, but not the ΔybtS culture supernatant. The data are presented as means ± SD of three independent experiments. (b) SOD activity is not observed in UTI89 or ΔybtS culture supernatants in the absence of copper. (c) A representative full scan mass spectrum of the active 80% methanol fraction from copper-treated UTI89 supernatant reveals the presence of Cu(II)-Ybt at m/z 543.

changed between controls and the complete xanthine/xanthine oxidase system. These findings are consistent with a catalytic rather than consumptive mode of superoxide degradation.

To further differentiate between superoxide consumption *versus* catalytic cycling through reactions 1 and 2, we quantified hydrogen peroxide produced during this reaction (Figure 4c). H_2O_2 is a superoxide dismutation reaction product that would not be generated if Cu(II)-Ybt is irreversibly consumed during the reaction with superoxide anion, as might conceivably occur if Cu(I)-Ybt were a stable product. In the xanthine/xanthine oxidase system, H_2O_2 concentrations were significantly higher (p = 0.0067, t test) in the reaction with Cu(II)-Ybt (0.04 μM) than with *apo*-Ybt or control. This result further supports the proposed catalytic mode of superoxide degradation in which a second superoxide oxidatively regenerates Cu(II)-Ybt.

Ybt's SOD-Like Activity Requires a Complexed, Redox Active Metal. To determine the effect of omitting copper or substituting other Ybt metal ligands, we assessed the superoxide dismutase-like activity of *apo*-Ybt, ferric-Ybt (Fe(III)-Ybt), and gallium-Ybt (Ga(III)-Ybt) and compared it to that of Cu(II)-Ybt (Figure 4b). Catalytic activity was in the order Cu(II)-Ybt > Fe(III)-Ybt ≫ Ga(III)-Ybt, a trend that reflects the activities for equimolar quantities of the corresponding metal salts. The negligible activity of Ga(III)-Ybt is consistent with gallium's inability to participate in biological redox cycling reactions. Cu(II)-Ybt exhibited the highest activity, suggesting that Ybt-secreting bacteria not only sequester phagolysosomal copper but also use it to help resist the respiratory burst.

Ybt's Heterocyclic Ring System Maintains SOD-Like Activity. Cu(II)-Ybt SOD-like activity may parallel that described for synthetically generated Cu(II)-salicylate complexes.[23] To determine the structure–function relationship between Ybt's salicylate and non-salicylate constituents, we compared superoxide dismutase-like activity of Cu(II) in the presence of salicylate (SA) or Ybt (Figure 5a). Both SA and Ybt enhanced the SOD-like activity of Cu(II) to a similar degree, consistent with activity enhancement from phenolate coordination. Competitive Cu(II) binding by physiologically plausible protein concentrations greatly attenuates the SOD-like activity of Cu(II)-SA complexes. To determine if Cu(II)-Ybt's activity is similarly limited, we repeated the above experiments in the presence of 1.0 mg/mL bovine serum albumin (BSA). Whereas BSA strongly attenuated the SOD-like activity of Cu(II)-SA as previously reported, Cu(II)-Ybt activity was unaffected (Figure 5b and c).

Proposed Cu(II)-Ybt Catalytic Model. Superoxide dismutation by copper-based catalysts involves two sequential reactions (see eqs 1 and 2 above. In this instance, M = Cu, n = 1). To develop a model for superoxide dismutation catalyzed by Cu(II)-Ybt, we used density function theory (DFT) to simulate Cu(II)-Ybt complexes and their interactions with superoxide. Simulated Cu(II)-Ybt structures predict two closely related linkage isomers (Figure 6a) with a common square planar metal coordination core, which is in agreement with experimental ion fragmentation data (Supplemental Figure S5). Cu(II) coordination by the salicylate oxygen and the ring 2 thiazole nitrogen is common to both linkage isomers, and these bonds are retained upon superoxide binding (Figure 6b). Subsequent Cu(II) reduction by superoxide (accompanied by the loss of dioxygen) yields species A_{0B}, a tridentate cuprous complex with two long-bond metal interactions. Complexation with the second superoxide displaces all interactions except those with the salicylate oxygen and ring 2 thiazole nitrogen coordinating groups to form the tridentate unit A_{0C}. Superoxide reduction and protonation releases H_2O_2 and restores the original complex. Stepwise complexation, superoxide dismutation, and subsequent H_2O_2 dissociation are accompanied by a favorable net negative total enthalpic contribution (predicted $^2H_{rxn,cyc}$= −31.3 kcal/mol). These simulations support Ybt as a

dx.doi.org/10.1021/cb400658k | ACS Chem. Biol. 2014, 9, 551–561

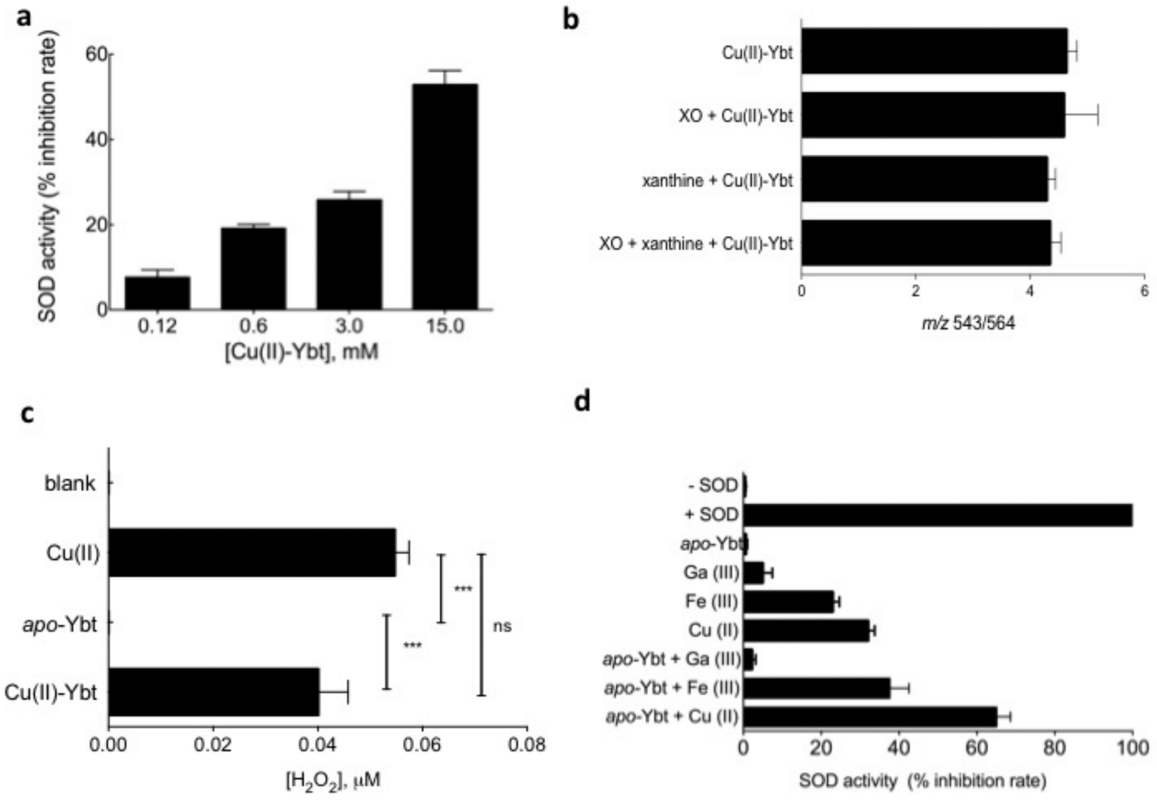

Figure 4. Cu(II)-Ybt is a superoxide dismutase mimic. Superoxide's interaction with Cu(II)-Ybt was probed *in vitro* with the superoxide-generating xanthine/xanthine oxidase (XO) reaction system. (a) A dose−response relationship is observed between Cu(II)-Ybt and SOD activity. (b) Cu(II)-Ybt concentrations remain unchanged following exposure to the intact xanthine/xanthine oxidase system. (c) In a complete reaction system, 10 μM Cu(II)-Ybt generates 0.04 μM hydrogen peroxide (H_2O_2) in the presence of superoxide anion, which is significantly (p = 0.0067, Mest) higher than the H_2O_2 generated in the presence of apo-Ybt alone or the negative control. (d) SOD ctivify is negligible for apo-Ybt alone but 63.12% and 41.4% for its Cu(II) andFe(III) complexes, respectively. This activity is absent in complexes with the redox-inactive metal Ga(III). Results are reported as a normalized percentage compared to positive controls treated with bovine superoxide dismutase. The data are presented as means ± SD of five independent experiments.

hemilabile ligand able to retain its association with a redox cycling Cu(II) ion while interacting with superoxide anions.

Our results demonstrate that Ybt expression protects intracellular uropathogenic *E. coli* from the respiratory burst following phagocytosis in two different macrophage cell types. This protective function requires copper ions, which spontaneously form stable Cu(II)-Ybt complexes with superoxide dismutase-like activity (Figure 7). Key features of this complex are its redox-active copper center, a phenolate-metal interaction, and an extended heterocyclic chain that permits catalytic activity while maintaining copper-coordination in protein-rich environments. Ybt emerges from these studies as a multifunctional virulence-associated secondary metabolite capable of forming a non-protein, copper-centered catalyst that helps bacteria resist the respiratory burst of activated phagocytes.

The intraphagosomal space surrounding internalized *E. coli* confines secreted host and pathogen molecules within a very small volume (~1.2×10^{-15} L),[40] resulting in local molar concentrations much higher than those achieved in our *in vitro* experimental systems. While peak steady state superoxide concentrations in the xanthine/xanthine oxidase system are <1 μM,[41] steady state phagosomal superoxide concentrations have been determined to exceed 100 μM.[40,42] Product levels in minimal media cultures suggest that mid- to high-millimolar Ybt may accumulate intraphagosomally within 1 h. As a second order disproportionation reaction with respect to superoxide,[43] intraphagosomal Cu(II)-Ybt-catalyzed dismutation is expected to proceed at a far greater rate than *in vitro* xanthine/xanthine oxidase-based reactions.

Although Cu,Zn-SOD is the most efficient (k_{cat}/K_m) enzyme known and exhibits an approximately 20-fold higher molar activity than Cu(II)-Ybt, the Ybt-based catalyst offers several potential advantages to pathogens. Its biosynthetic cost is lower (0.5 kD complex *vs* >15 kD protein), resulting in lower metabolic costs to a nutritionally stressed pathogen. Furthermore, because Cu(II)-Ybt's peptide bonds are condensed to protease-resistant thiazoline and thiazolidine rings, it would be expected to survive the protease-rich phagosome far longer than a protein-based catalyst.[44] Indeed, Kim *et al.* showed that a Cu,Zn-SOD with greater protease resistance more effectively protected Salmonella from phagosomal killing than protease-sensitive Cu,Zn-SOD.[45] Ybt expression may thus be a specialized defense against phagocytic killing.

The precise nature of microbial protection from extracellular superoxide remains unclear. NADPH-derived superoxide anions do not cross membranes, suggesting that the relevant interactions occur outside the bacterial cytoplasm and are unaffected by cytoplasmic SODs. In the presence of phagosomal copper ions, it is possible that NADPH oxidase-derived superoxide reduces Cu(II) (eq 3), generating a more freely diffusible toxic cuprous (Cu(I)) species that can displace

dx.doi.org/10.1021/cb400658k | *ACS Chem. Biol.* 2014, 9, 551−561

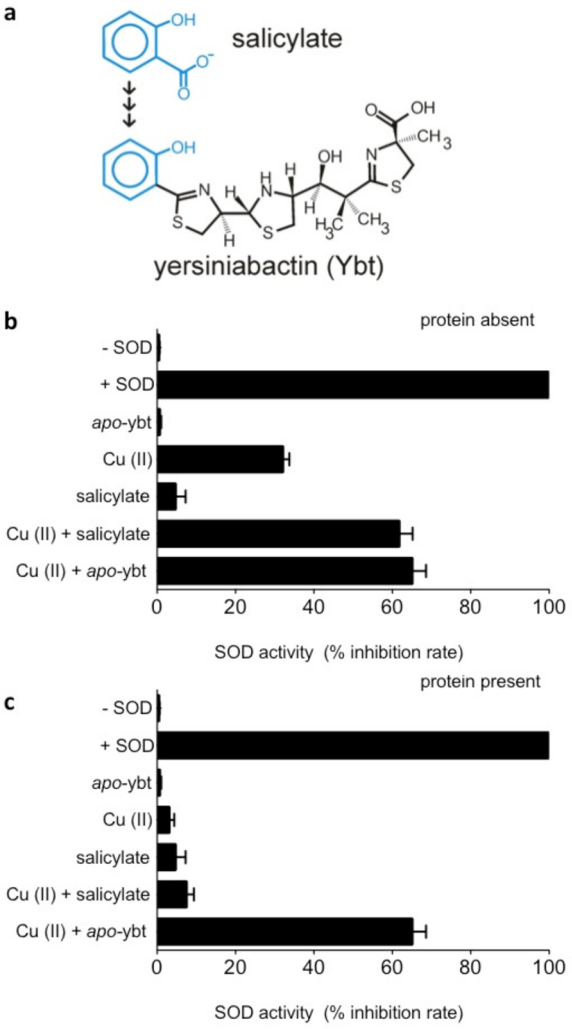

Figure 5. SOD activity of Cu(II)-Ybt is selectively retained in the presence of protein. (a) Salicylate is modified by nonribosomal peptide transferase/polyketide synthase proteins in bacterial pathogens to synthesize Ybt. (b) Superoxide-dismutase activities of Cu(II), salicylate, and Ybt alone and in combination were determined. SOD activity determined for Cu(II)-salicylate complexes is 61.6%, similar to the 65% determined for Cu(II)-Ybt complexes. (c) SOD activities of these complexes were measured in the presence of 1.0 mg/mL protein [bovine serum albumin (BSA)] to determine whether activity is retained in a more physiologically relevant environment with high concentration of protein. BSA quenched the superoxide dismutase activity associated with Cu(II)-salicylate complexes but not that associated with Cu(II)-Ybt complexes. This functional preservation suggests an additional biochemical rationale for the extended salicylate modification by yersiniabactin biosynthetic proteins.

iron from bacterial iron–sulfur cluster proteins.[46] Indeed, Cu(II) reduction is observed to significantly enhance copper toxicity to UTI89. Whether copper toxicity is ultimately attributable to Cu(I) or occurs indirectly through Fenton-like chemistry remains unclear (eqs 3 and 4).[47]

$$Cu(II) + O_2^{\bullet -} \rightarrow Cu(I) + O_2 \quad (3)$$

$$Cu(I) + H_2O_2 \rightarrow Cu(II) + OH^- + OH^{\bullet} \quad (4)$$

In either scenario, Ybt's ability to both sequester extracellular Cu(II) and catalyze superoxide dismutation provides a possible rationale for its ability to protect intracellular uropathogens.

Cu(II)-Ybt's SOD activity may facilitate bacterial survival in multiple pathologically significant environments. Protein superoxide dismutases are recognized virulence-associated factors in an array of bacterial and fungal pathogens known to occupy intracellular locations in the host.[48−51] Phagocyte-rich lymphatic tissue is a common pathophysiologic niche for pathogenic *Yersiniae*, which carry Ybt biosynthetic genes. Although not classically recognized as an intracellular pathogen, uropathogenic *E. coli* exhibit enhanced macrophage survival relative to non-pathogenic strains, which may facilitate intracellular persistence.[52] Less clear is whether Ybt influences intracellular survival in non-professional phagocytic cells such as bladder epithelial cells, where UPEC have been described to establish intracellular reservoirs. Although urinary epithelial cells express the non-phagocyte-associated NADPH oxidase Duox1, its impact on urinary tract pathogenesis or bacterial colonization remains unclear.[53]

It is notable that synthetic SOD mimics have been the goal of multiple synthetic efforts for several decades (see review, ref 54). Although they span a broad range of ligands and metals, these mimics share the same metal-centered redox cycling catalytic mechanism identified for protein SODs. As with Cu(II)-Ybt, early SOD mimics were based on Cu(II)-SA complexes. These complexes were limited by low formation constants and instability in the presence of competitive metal chelators, which are highly abundant in physiologic systems. The natural products Ybt and methanobactin[55−58] appear to have solved this limitation by incorporating multiple heteroaromatic rings that maintain copper coordination while permitting superoxide interactions. Natural products such as these may provide useful insights for synthetic SOD mimics.

Ybt's ability to bind copper and act as a catalyst shows how the chemical diversity characteristic of microbial siderophores may manifest not only in ferric ion binding and acquisition, but also as additional, idiosyncratic interactions with other metal ions and host factors. Other microbial siderophores and natural products may perform additional enzymatic or catalytic functions that offer important advantages over enzymes in certain host microenvironments. A greater understanding of microbial secondary product chemistry and the environments associated with their expression may uncover previously unappreciated virulence-associated functions.

METHODS

Bacterial Strains and Cultivation. UTI89, a well-characterized and fully sequenced uropathogenic *E. coli* strain, was used as the prototypic pathogen in this study.[2,59] UTI89::kan was constructed by inserting a kanamycin resistance cassette into the HK phage attachment site using previously described methods.[60] UTI89 mutant strains used in this study are listed in Supplemental Table 1. Bacterial cultures were grown from a single colony in Difco Luria–Bertani broth, Miller (LB) (Beckton Dickinson) for 3 h and subsequently diluted 1:100 into M63 medium supplemented with 0.2% v/v glycerol and 10 mg/mL niacin (Sigma). Bacterial cultures were incubated for 18 h at 37 °C in a rotary shaker. UTI89 with a kanamycin resistance cassette was grown in 50 μg/mL antibiotic when appropriate. Antibiotic resistant strains were selected on LB-kanamycin (100 μg/mL) plates.

Deletion-Strain Construction. In-frame deletions in UTI89 were made using the lamba Red recombinase method, as previously described, using pKD4 or pKD13 as a template.[60,61] To confirm the appropriate deletions, we performed PCR with flanking primers. Antibiotic resistance insertions were removed by transforming the mutant strains with pCP20 expressing the FLP recombinase.

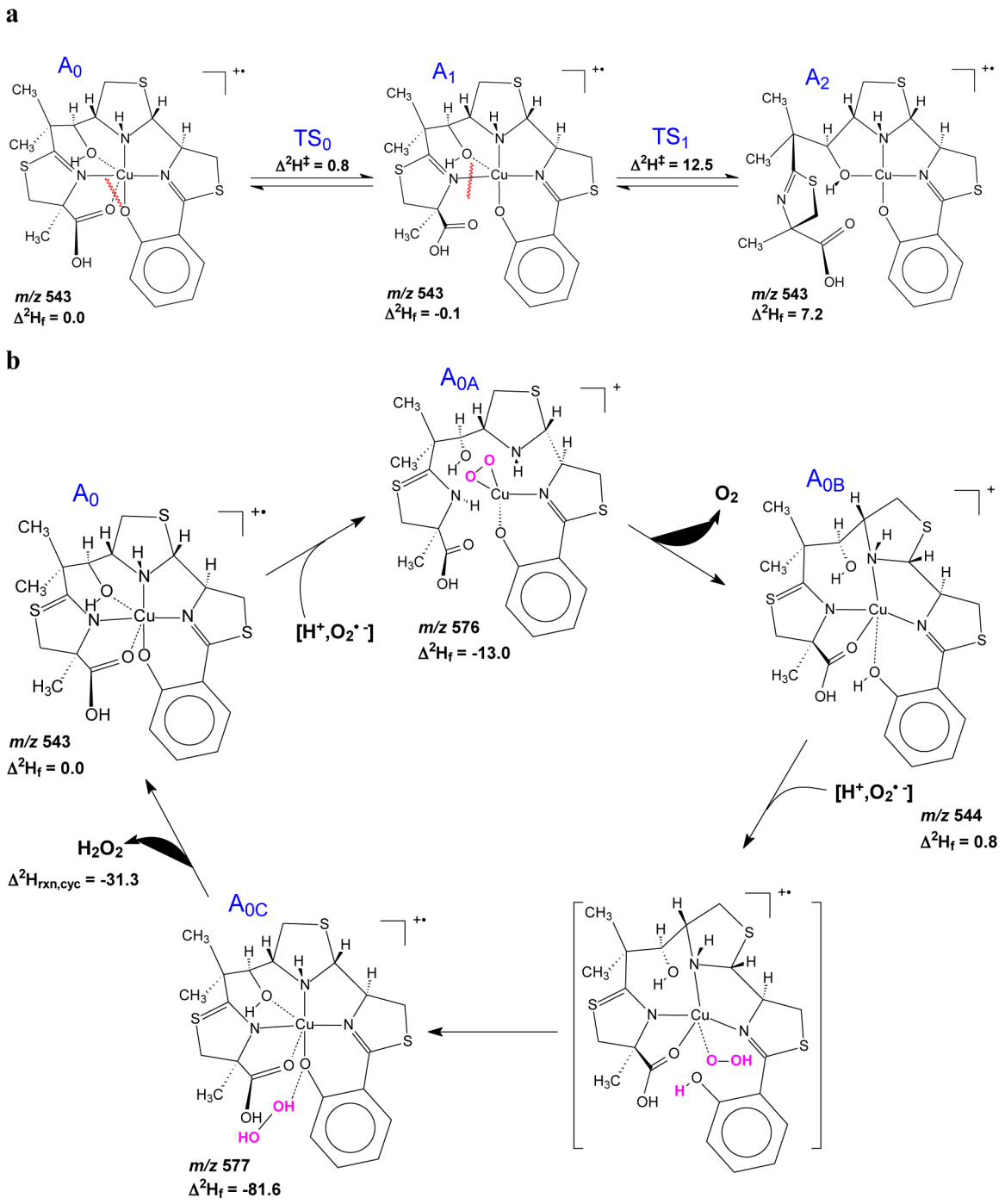

Figure 6. DFT model of superoxide dismutation catalysis by Cu(II)-Ybt. (a) The energetically most-favored structures of m/z 543, A_0, A_1, and A_2, are associated with relative calculated enthalpies of formation of 0.0, −0.1, and 7.3 kcal/mol, respectively. (b) Redox cycling of Cu(II)-Ybt as a basis for SOD activity. Structural predictions based on DFT calculations of possible superoxide adducts start from the most stable form of the Cu(II) complex, A_0 (m/z 543, Δ^2H_f = 0.0 kcal/mol). Upon binding the first superoxide and a proton, Cu(II) releases all interactions except those with the salicylate O and ring 2N, forming a distorted square planar unit with the oxygens from the O_2 moiety, A_{0A} (m/z 576, Δ^2H_f = −13.0 kcal/mol). Release of O_2 followed by proton transfer to the salicylate O yields a Cu(I) species, A_{OB} (m/z 544, Δ^2H_f = 0.8 kcal/mol), which forms a distorted square-planar species with long-bond interactions. Upon addition of the second superoxide with a proton, this species forms an unstable pentadentate unit about Cu(I), which yields A_{OC} (m/z 577, Δ^2H_f = −81.6 kcal/mol) upon proton transfer. In this complex, the nascent hydrogen peroxide unit is held in a pocket by hydrogen bonding before its dissociation restores the original complex ($\Delta^2H_{rxn,cyc}$ = −31.3 kcal/mol).

Chemicals and Reagents. Methanol (HPLC grade) and water (HPLC grade) were purchased from Fisher Scientific (Fisher Scientific). Salicylic acid, cupric sulfate, ferric chloride, gallium nitrate, diphenyleneiodonium chloride (DPI), and bovine serum albumin (BSA) were purchased from Sigma (Sigma-Aldrich Corporation). Superoxide assay kit (CAT19160) and catalase assay kits (CAT 100) were purchased from Sigma (Sigma-Aldrich Corporation).

Yersiniabactin Isolation and Characterization. ferric chloride or copper sulfate (1.0 M) was added to UTI89Δ*entB* cell culture supernatants to a final concentration of 50 mM and metal-Ybt complexes were purified as described previously. The supernatant from

dx.doi.org/10.1021/cb400658k | ACS Chem. Biol. 2014, 9, 551−561

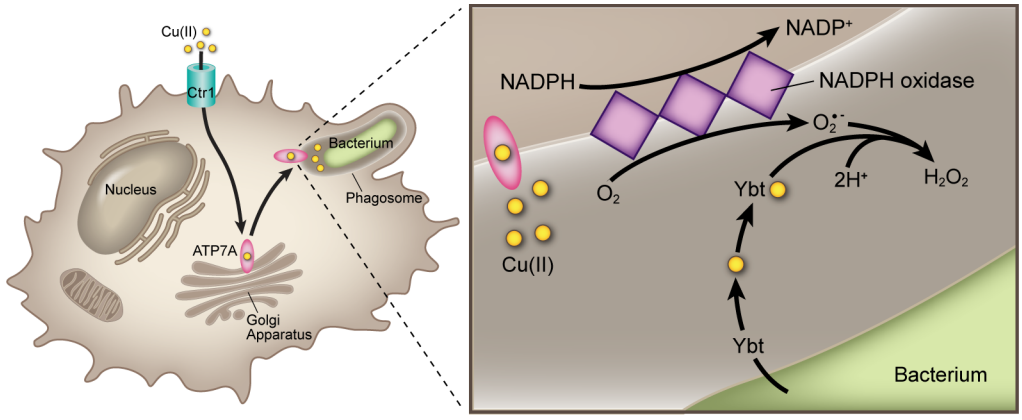

Figure 7. Model for the interaction between Cu(II) and Ybt within the phagosome. In activated macrophages, host ATP7A secretes copper into the phagosomal compartment enclosing internalized bacteria. Superoxide anions ($O_2^{\bullet-}$) are generated within this compartment by NADPH oxidase. Ybt secreted by intraphagosomal bacteria spontaneously interacts with Cu(II) to form Cu(II)-Ybt. Cu(II)-Ybt's SOD-like activity diminishes steady state superoxide concentration. By complexing free copper and minimizing superoxide levels, yersiniabactin reduces levels of toxic Cu(I) or other redox-active toxins.

this precipitation reaction was clarified by centrifugation and subsequently subjected to preparative chromatography, eluted with 100% methanol. The presence of cupric- and ferric-yersiniabactin was confirmed by LC−MS detection of these complexes at m/z 543 and 535, respectively.

Tissue Culture. RAW264.7 cells were obtained from the American Type Culture Collection and maintained in Gibco's RPMI 1640 medium (Invitrogen) containing 10% v/v fetal bovine serum (Invitrogen) in 5% CO_2 at 37 °C.

Bacterial Survival within RAW 264.7 Macrophages. RAW264.7 macrophages were detached from TPP cell culture flasks by scraping into ice-cold medium containing 10% v/v FBS, washed twice, and resuspended in 24-well plates at 10^5 cells/well. The seeded wells were treated in the following order: 24 h in (i) ice-cold media containing 10% v/v FBS, followed by a 24 h incubation in (ii) serum-free media, followed by a 24 h incubation in (iii) serum-free media either with or without 20 μM $CuSO_4$. Wild type *E. coli* (strain UTI89), isogenic mutants Δ*ybtS*, Δ*fyuA*, Δ*fyuA*Δ*ybtS*, *E. coli* harboring a resistance cassette to kanamycin (strain UTI89::kan), or MG1655 were grown for 18 h to stationary phase in M63 minimal media and added to the RAW264.7 macrophages at a multiplicity of infection (MOI; macrophage/bacteria ratio) of 1:10 or 1:1. Each experimental condition was set up in triplicate wells. Bacterial phagocytosis was allowed to proceed for 30 min at 37 °C. At 30 min, one set of samples (total inoculum) was lysed in 0.1% v/v Triton X-100 solution and plated onto LB-agar plates for CFU enumeration to provide total bacterial inoculum. A second set (uptake group) was washed 4 times with 1× ice-cold PBS to wash extracellular bacteria, lysed with serum-free media containing 0.1% v/v Triton X-100, and plated as described above. A third set of samples (kill group) was treated with serum-free media containing 100 μg/mL gentamicin (Invitrogen) and incubated for 1 h to allow bacterial killing to occur in the RAW264.7 cells. Following this incubation period, the samples were washed 4 times with 1× PBS to remove extracellular gentamicin, then lysed with 0.1% v/v Triton, and plated onto LB-agar. Bacterial survival was determined as the ratio of CFU in the killing group over CFU of the uptake group.

In mixed infections, bacterial cultures were mixed in equal optical densities to prepare the mixed inoculum. Total CFU was determined from LB plates, and the number of kanamycin-resistant (UTI89::kan) CFU was determined for bacteria that grew on LB-kanamycin (100 μg/mL) plates. Competition indices (CI) were calculated by using UTI89::kan as the reference strain as follows: CI = ($CFU_{UTI89::kan}$/CFU_{mutant} recovered from RAW264.7 cells)/($CFU_{UTI89::kan}$/CFU_{mutant} present in the initial inoculum).[62]

Inhibition of Oxygen-Dependent Innate Activity of RAW264.7 Cells. Diphenyleneiodonium (DPI) produces a non-competitive inhibition of NADPH oxidase by its covalent binding to FAD.[63] RAW264.7 macrophages were infected with bacteria as described above, and samples were treated with 20 μM DPI (Sigma). Samples containing media alone, media with 20 μM copper, or media with both 20 μM copper and 20 μM DPI were used as additional controls. Reduction in NADPH oxidase activity was observed by treating samples with 20 μM NBT and a microtiter plate was used to determine the corresponding change in absorbance at 560 nm.

Bacterial Survival within Peritoneal Resident Macrophages. C57BL/6 and X-CGD ($gp91^{phox-/-}$) mice were a kind gift of Dr. Mary C. Dinauer at Washington University School of Medicine in Saint Louis. All mice received care in accordance with the institutional guidelines. Female mice between 8 and 16 weeks of age provided a source of resident peritoneal macrophages. Briefly, mice were euthanized with CO_2, and the peritoneal cavity of each mouse was lavaged with 10 mL of PBS with 1 mM EDTA. Cells were collected, centrifuged at 1,200 rpm for 10 min, and resuspended in RPMI supplemented with 20% v/v FBS. Then 125,000 total lavage cells were plated in 18-well tissue culture plates and incubated at 37 °C for 2 h. After 2 h of culture, non-adherent cells were aspirated, wells were washed once with ice-cold 1× PBS, and prewarmed RPMI with 20% v/v FBS was added to each well. Absolute cell numbers were obtained using a Coulter counter (Coulter Channelyzer 256).

UTI89::kan, Δ*ybtS*, or Δ*fyuA* were inoculated at 1:1000 from LB starter cultures into M63 minimal media and grown for 6 h to mid-log phase at 37 °C with shaking. Cell cultures were normalized and co-inoculated to the resident peritoneal macrophages at a MOI of 1:10. Bacterial phagocytosis was allowed to proceed for 30 min at 37 °C. At 30 min, macrophage sets (total inoculum and adherent group) were treated similarly as the RAW246.7 cell protocol outlined above. The kill group was incubated for 30 min following treatment with serum-free media containing 100 μg/mL gentamicin. Bacteria were plated, and competitive indices calculated as described above.

Superoxide Dismutase Activity. Superoxide dismutase (SOD) activity was measured indirectly in multiwell plates, using xanthine/xanthine oxidase as the superoxide-generating system and the reduction of Dojindo's highly water-soluble tetrazolium salt, WST-1 (2-(4-Iodophenyl)- 3-(4-nitrophenyl)-5-(2,4-disulfophenyl)-2*H*-tetrazolium, monosodium salt) to produce a water-soluble formazan dye as the detector (Sigma-19160). Reduction of WST-1 was monitored at 440 nm in a final volume of 100 μL. Percent inhibition rate was defined as the amount of compound that blocked WST-1 reduction, normalized to the inhibition observed in the control buffers. Bovine Cu,Zn-SOD was used as a standard (Sigma S-7571). Controls for the SOD assay included ensuring that the compound did not affect the superoxide-generating reaction, testing solvent alone, and ensuring that the compound does not react independently with WST-1. To

dx.doi.org/10.1021/cb400658k | *ACS Chem. Biol.* 2014, 9, 551−561

determine whether SOD activity is retained in the presence of protein, these experiments were repeated in the presence of 1.0 mg/mL bovine serum albumin (Sigma).

Mass Spectrometry and Spectrophotometry of Yersiniabactin in the Presence of Superoxide Anion. The SOD activity assay reagents (Sigma) described above was adapted to determine the effects of superoxide anion on the yersiniabactin backbone and the Cu(II)-Ybt complex. Aliquots (200 μL) of 10 μM copper sulfate, *apo*-Ybt, or Cu(II)-Ybt were exposed to the xanthine/xanthine oxidase reaction system. Since WST-1 reacts with free superoxide anions, it was not added to any reaction mixture. The reaction was allowed to proceed for 20 min at 37 °C. Following incubation, 10 μL of ^{13}C-labeled internal standard was added to a 150-μL aliquot of each sample, and the samples were subjected to preparative chromatography. The ratio of labeled to unlabeled Cu(II)-Ybt was determined in each sample as described previously by Chaturvedi *et al.*[8]

Hydrogen Peroxide Quantification. Aliquots (1 mL) of 10 μM copper, Cu(II)-Ybt, and appropriate SOD reaction substrates (defined above) were allowed to incubate for 15 min, and the reaction was stopped using the catalase assay stop solution (15 mM sodium azide in buffer). H_2O_2 levels in each reaction vial were determined by adapting a catalase assay reagents (Cat-100, Sigma). This assay is normally deployed to determine H_2O_2 levels following catalase activity using a colorimetric substrate. This colorimetric method uses a subsituted phenol (3,5-dichloro-2-hydroxybenzene-sulfonic acid), which couples oxidatively to 4-aminoantipyrine in the presence of H_2O_2 and horseradish peroxidase (HRP) to give a red quinoneimine dye (*N*-(4-antipyryl)-3-chloro-5-sulfonate-p-benzoquinone-monoimine) that absorbs at 520 nm. H_2O_2 standard (Sigma) was used to generate a standard curve to calibrate this reaction (Supplemental Figure S6).

High-Resolution Liquid Chromatography−Mass Spectrometry. High-resolution mass spectrometry analyses of cupric- and ferric-yersiniabactin complexes were conducted using a Bruker Maxis Q-Tof operated in positive ion mode as previously described. The samples were directly infused at a flow rate of 0.3 μL/min. The ion spray voltage was set to 4500 V for positive ion and −500 V for negative ion mode, respectively. The nebulizer gas (air) and turbo gas (air) were set to 0.4 bar and 4.0 L/min, respectively. The heater temperature was 180 °C.

Theoretical Calculations. Theoretical calculations were performed to characterize the potential-energy surface (PES) associated with fragmentation and reaction. Conformer spaces for precursors (cupric and ferric complexes with Ybt), and intermediates were explored by Monte Carlo/MMFF molecular mechanisms/dynamics methods. From these results, structures of precursors, intermediates, and scans for associated transition states were explored by using the PM3 semiempirical algorithm,[64] both in Spartan[65] for Linux v. Two (Wave function, Inc.). DFT (Density Functional Theory, part of Gaussian 03 and 09 suites, Gaussian Inc.) calculations were performed by using the PBE0 functional[66,67] (PBE1PBE in Gaussian parlance) with basis sets Def2-SVP and Def2-TZVP.[68] Minima and transition states were optimized at the level PBE1PBE/Def2-SVP and confirmed by vibrational frequency analysis. In addition, connections of transition states to minima were examined by inspection, projections along normal reaction coordinates, and path calculations as necessary. Single-point energies were calculated at level PBE1PBE/Def2-TZVP, and scaled thermal-energy corrections were applied using scaling factors for B3LYP/6-31G(d,p).[69] Solvent-based interactions were calculated at the same level by using the CPCM polarizable conductor calculation model for water and using the Universal Force Field for atomic radii. The hybrid functional and basis sets were chosen on the basis of performance with transition metal complexes.[70,71] DFT was selected for high-level calculations on pragmatic reasons because it requires overall less computational overhead than *ab initio* methods and performs adequately.[72−74] All results are reported in kcal/mol as enthalpies of formation relative to a selected, suitable precursor. The complexes are all radicals because of the transition-metal cation involved. The Cu(II) complexes are spin 1/2 with the Cu(II) in low-spin.

Statistical Analyses. Statistics and graphs were generated using GraphPad Prism 4 (GraphPad software). Student's *t* test was used to compare growth differences between paired strains. Analyses of paired intracellular survival differences in competitive co-infections were performed using the Wilcoxon signed-rank test for significance.

■ ASSOCIATED CONTENT

Ⓢ Supporting Information

This material is available free of charge *via* the Internet at http://pubs.acs.org.

■ AUTHOR INFORMATION

Corresponding Author

*E-mail: jhenderson@DOM.wustl.edu.

Notes

The authors declare no competing financial interest.

■ ACKNOWLEDGMENTS

J.P.H. holds a Career Award for Medical Scientists from the Burroughs Wellcome Fund. We acknowledge NIH grants K12 HD001459-09, P30 HL101263-01, and P50 DK64540. Mass spectrometry was supported by NIH grants P41-RR00954, P60-DK20579, and P30-DK56341 and by the Washington University Computational Chemistry Facility, supported by NSF grant #CHE-0443501. We thank the Children's Discovery Institute of Washington University and St. Louis Children's Hospital on behalf of M. Dinauer.

■ REFERENCES

(1) Miethke, M., and Marahiel, M. A. (2007) Siderophore-based iron acquisition and pathogen control. *Microbiol. Mol. Biol. Rev. 71*, 413−451.

(2) Chen, S. L., Hung, C. S., Xu, J., Reigstad, C. S., Magrini, V., Sabo, A., Blasiar, D., Bieri, T., Meyer, R. R., Ozersky, P., Armstrong, J. R., Fulton, R. S., Latreille, J. P., Spieth, J., Hooton, T. M., Mardis, E. R., Hultgren, S. J., and Gordon, J. I. (2006) Identification of genes subject to positive selection in uropathogenic strains of Escherichia coli: a comparative genomics approach. *Proc. Natl. Acad. Sci. U.S.A. 103*, 5977−5982.

(3) Henderson, J. P., Crowley, J. R., Pinkner, J. S., Walker, J. N., Tsukayama, P., Stamm, W. E., Hooton, T. M., and Hultgren, S. J. (2009) Quantitative metabolomics reveals an epigenetic blueprint for iron acquisition in uropathogenic Escherichia coli. *PLoS Pathog. 5*, e1000305.

(4) Snyder, J. A., Haugen, B. J., Buckles, E. L., Lockatell, C. V., Johnson, D. E., Donnenberg, M. S., Welch, R. A., and Mobley, H. L. (2004) Transcriptome of uropathogenic Escherichia coli during urinary tract infection. *Infect. Immun. 72*, 6373−6381.

(5) Bachman, M. A., Oyler, J. E., Burns, S. H., Caza, M., Lepine, F., Dozois, C. M., and Weiser, J. N. (2011) Klebsiella pneumoniae yersiniabactin promotes respiratory tract infection through evasion of lipocalin 2. *Infect. Immun. 79*, 3309−3316.

(6) Mokracka, J., Koczura, R., and Kaznowski, A. (2004) Yersiniabactin and other siderophores produced by clinical isolates of Enterobacter spp. and Citrobacter spp. *FEMS Immunol. Med. Microbiol. 40*, 51−55.

(7) Carniel, E. (1999) The Yersinia high-pathogenicity island. *Int. Microbiol. 2*, 161−167.

(8) Chaturvedi, K. S., Hung, C. S., Crowley, J. R., Stapleton, A. E., and Henderson, J. P. (2012) The siderophore yersiniabactin binds copper to protect pathogens during infection. *Nat. Chem. Biol. 8*, 731−736.

(9) Hodgkinson, V., and Petris, M. J. (2012) Copper homeostasis at the host-pathogen interface. *J. Biol. Chem. 287*, 13549−13555.

(10) Swain, B. K., Talukder, G., and Sharma, A. (1980) Genetic variations in serum proteins in relation to diseases. *Med. Biol. 58*, 246–263.
(11) Chiarla, C., Giovannini, I., and Siegel, J. H. (2008) Patterns of correlation of plasma ceruloplasmin in sepsis. *J. Surg. Res. 144*, 107–110.
(12) Natesha, R. K., Natesha, R., Victory, D., Barnwell, S. P., and Hoover, E. L. (1992) A prognostic role for ceruloplasmin in the diagnosis of indolent and recurrent inflammation. *J. Natl. Med. Assoc. 84*, 781–784.
(13) Beveridge, S. J., Garrett, I. R., Whitehouse, M. W., Vernon-Roberts, B., and Brooks, P. M. (1985) Biodistribution of 64Cu in inflamed rats following administration of two anti-inflammatory copper complexes. *Agents Actions 17*, 104–111.
(14) Voruganti, V. S., Klein, G. L., Lu, H. X., Thomas, S., Freeland-Graves, J. H., and Herndon, D. N. (2005) Impaired zinc and copper status in children with burn injuries: need to reassess nutritional requirements. *Burns 31*, 711–716.
(15) Jones, P. W., Taylor, D. M., Williams, D. R., Finney, M., Iorwerth, A., Webster, D., and Harding, K. G. (2001) Using wound fluid analyses to identify trace element requirements for efficient healing. *J. Wound Care 10*, 205–208.
(16) Wagner, D., Maser, J., Lai, B., Cai, Z., Barry, C. E., 3rd, Honer Zu Bentrup, K., Russell, D. G., and Bermudez, L. E. (2005) Elemental analysis of Mycobacterium avium-, Mycobacterium tuberculosis-, and Mycobacterium smegmatis-containing phagosomes indicates pathogen-induced microenvironments within the host cell's endosomal system. *J. Immunol. 174*, 1491–1500.
(17) Crocker, A., Lee, C., Aboko-Cole, G., and Durham, C. (1992) Interaction of nutrition and infection: effect of copper deficiency on resistance to Trypanosoma lewisi. *J. Natl. Med. Assoc. 84*, 697–706.
(18) Ilback, N. G., Benyamin, G., Lindh, U., and Friman, G. (2003) Sequential changes in Fe, Cu, and Zn in target organs during early Coxsackievirus B3 infection in mice. *Biol. Trace Elem. Res. 91*, 111–124.
(19) Matousek de Abel de la Cruz, A. J., Burguera, J. L., Burguera, M., and Anez, N. (1993) Changes in the total content of iron, copper, and zinc in serum, heart, liver, spleen, and skeletal muscle tissues of rats infected with Trypanosoma cruzi. *Biol. Trace Elem. Res. 37*, 51–70.
(20) Tufft, L. S., Nockels, C. F., and Fettman, M. J. (1988) Effects of Escherichia coli on iron, copper, and zinc metabolism in chicks. *Avian Dis. 32*, 779–786.
(21) La Fontaine, S., Ackland, M. L., and Mercer, J. F. (2010) Mammalian copper-transporting P-type ATPases, ATP7A and ATP7B: emerging roles. *Int. J. Biochem. Cell Biol. 42*, 206–209.
(22) White, C., Lee, J., Kambe, T., Fritsche, K., and Petris, M. J. (2009) A role for the ATP7A copper-transporting ATPase in macrophage bactericidal activity. *J. Biol. Chem. 284*, 33949–33956.
(23) Darr, D., Zarilla, K. A., and Fridovich, I. (1987) A mimic of superoxide dismutase activity based upon desferrioxamine B and manganese(IV). *Arch. Biochem. Biophys. 258*, 351–355.
(24) Palazzolo-Ballance, A. M., Suquet, C., and Hurst, J. K. (2007) Pathways for intracellular generation of oxidants and tyrosine nitration by a macrophage cell line. *Biochemistry 46*, 7536–7548.
(25) VanderVen, B. C., Yates, R. M., and Russell, D. G. (2009) Intraphagosomal measurement of the magnitude and duration of the oxidative burst. *Traffic 10*, 372–378.
(26) Pollock, J. D., Williams, D. A., Gifford, M. A., Li, L. L., Du, X., Fisherman, J., Orkin, S. H., Doerschuk, C. M., and Dinauer, M. C. (1995) Mouse model of X-linked chronic granulomatous disease, an inherited defect in phagocyte superoxide production. *Nat. Genet. 9*, 202–209.
(27) Yu, L., Cross, A. R., Zhen, L., and Dinauer, M. C. (1999) Functional analysis of NADPH oxidase in granulocytic cells expressing a delta488–497 gp91(phox) deletion mutant. *Blood 94*, 2497–2504.
(28) Ding, C., Kume, A., Bjorgvinsdottir, H., Hawley, R. G., Pech, N., and Dinauer, M. C. (1996) High-level reconstitution of respiratory burst activity in a human X-linked chronic granulomatous disease (X-CGD) cell line and correction of murine X-CGD bone marrow cells by retroviral-mediated gene transfer of human gp91phox. *Blood 88*, 1834–1840.
(29) Adams, L. B., Dinauer, M. C., Morgenstern, D. E., and Krahenbuhl, J. L. (1997) Comparison of the roles of reactive oxygen and nitrogen intermediates in the host response to Mycobacterium tuberculosis using transgenic mice. *Tuber. Lung Dis. 78*, 237–246.
(30) Becker, L., Liu, N. C., Averill, M. M., Yuan, W., Pamir, N., Peng, Y., Irwin, A. D., Fu, X., Bornfeldt, K. E., and Heinecke, J. W. (2012) Unique proteomic signatures distinguish macrophages and dendritic cells. *PLoS One 7*, e33297.
(31) Liu, Y., Zhang, X. D., and Lu, C. S. (1996) SOD-like activity of copper salicylate complex in Tween micellar systems. *Sheng Wu Hua Xue Yu Sheng Wu Wu Li Xue Bao (Shanghai) 28*, 38–42.
(32) Auer, D. E., Ng, J. C., and Seawright, A. A. (1990) Copper salicylate and copper phenylbutazone as topically applied anti-inflammatory agents in the rat and horse. *J. Vet. Pharmacol. Ther. 13*, 67–75.
(33) Korolkiewicz, Z., Hac, E., Gagalo, I., Gorczyca, P., and Lodzinska, A. (1989) The pharmacologic activity of complexes and mixtures with copper and salicylates or aminopyrine following oral dosing in rats. *Agents Actions 26*, 355–359.
(34) Walker, W. R. (1987) Copper salicylate compounds. *Med. J. Aust. 147*, 104–106.
(35) Okuyama, S., Hashimoto, S., Aihara, H., Willingham, W. M., and Sorenson, J. R. (1987) Copper complexes of non-steroidal antiinflammatory agents: analgesic activity and possible opioid receptor activation. *Agents Actions 21*, 130–144.
(36) Jacka, T., Bernard, C. C., and Singer, G. (1983) Copper salicylate as an anti-inflammatory and analgesic agent in arthritic rats. *Life Sci. 32*, 1023–1030.
(37) Beveridge, S. J., Walker, W. R., and Whitehouse, M. W. (1980) Anti-inflammatory activity of copper salicylates applied to rats percutaneously in dimethyl sulphoxide with glycerol. *J. Pharm. Pharmacol. 32*, 425–427.
(38) Peskin, A. V., and Winterbourn, C. C. (2000) A microtiter plate assay for superoxide dismutase using a water-soluble tetrazolium salt (WST-1). *Clin. Chim. Acta 293*, 157–166.
(39) Ukeda, H., Shimamura, T., Tsubouchi, M., Harada, Y., Nakai, Y., and Sawamura, M. (2002) Spectrophotometric assay of superoxide anion formed in Maillard reaction based on highly water-soluble tetrazolium salt. *Anal. Sci. 18*, 1151–1154.
(40) Winterbourn, C. C., Hampton, M. B., Livesey, J. H., and Kettle, A. J. (2006) Modeling the reactions of superoxide and myeloperoxidase in the neutrophil phagosome: implications for microbial killing. *J. Biol. Chem. 281*, 39860–39869.
(41) Craig, M., and Slauch, J. M. (2009) Phagocytic superoxide specifically damages an extracytoplasmic target to inhibit or kill Salmonella. *PLoS One 4*, e4975.
(42) Korshunov, S., and Imlay, J. A. (2006) Detection and quantification of superoxide formed within the periplasm of Escherichia coli. *J. Bacteriol. 188*, 6326–6334.
(43) Bielski BHJ, A. A. (1977) Mechanism of disproportionation of superoxide radicals. *J. Phys. Chem. 81*, 1048–1050.
(44) Walsh, C. T., Malcolmson, S. J., and Young, T. S. (2012) Three ring posttranslational circuses: insertion of oxazoles, thiazoles, and pyridines into protein-derived frameworks. *ACS Chem. Biol. 7*, 429–442.
(45) Kim, B., Richards, S. M., Gunn, J. S., and Slauch, J. M. (2010) Protecting against antimicrobial effectors in the phagosome allows SodCII to contribute to virulence in Salmonella enterica serovar typhimurium. *J. Bacteriol. 192*, 2140–2149.
(46) Macomber, L., and Imlay, J. A. (2009) The iron-sulfur clusters of dehydratases are primary intracellular targets of copper toxicity. *Proc. Natl. Acad. Sci. U.S.A. 106*, 8344–8349.
(47) Liochev, S. I. (1999) The mechanism of "Fenton-like" reactions and their importance for biological systems. A biologist's view. *Met. Ions Biol. Syst. 36*, 1–39.
(48) Vanaporn, M., Wand, M., Michell, S. L., Sarkar-Tyson, M., Ireland, P., Goldman, S., Kewcharoenwong, C., Rinchai, D.,

Lertmemongkolchai, G., and Titball, R. W. (2011) Superoxide dismutase C is required for intracellular survival and virulence of Burkholderia pseudomallei. *Microbiology 157*, 2392−2400.
(49) Youseff, B. H., Holbrook, E. D., Smolnycki, K. A., and Rappleye, C. A. (2012) Extracellular superoxide dismutase protects histoplasma yeast cells from host-derived oxidative stress. *PLoS Pathog.*, 8.
(50) Raynaud, C., Etienne, G., Peyron, P., Laneelle, M. A., and Daffe, M. (1998) Extracellular enzyme activities potentially involved in the pathogenicity of Mycobacterium tuberculosis. *Microbiology 144* (Pt 2), 577−587.
(51) Gee, J. M., Valderas, M. W., Kovach, M. E., Grippe, V. K., Robertson, G. T., Ng, W. L., Richardson, J. M., Winkler, M. E., and Roop, R. M. (2005) The Brucella abortus Cu,Zn superoxide dismutase is required for optimal resistance to oxidative killing by murine macrophages an wild-type virulence in experimentally infected mice. *Infect. Immun. 73*, 2873−2880.
(52) Bokil, N. J., Totsika, M., Carey, A. J., Stacey, K. J., Hancock, V., Saunders, B. M., Ravasi, T., Ulett, G. C., Schembri, M. A., and Sweet, M. J. (2011) Intramacrophage survival of uropathogenic Escherichia coli: differences between diverse clinical isolates and between mouse and human macrophages. *Immunobiology 216*, 1164−1171.
(53) Donko, A., Ruisanchez, E., Orient, A., Enyedi, B., Kapui, R., Peterfi, Z., de Deken, X., Benyo, Z., and Geiszt, M. (2010) Urothelial cells produce hydrogen peroxide through the activation of Duox1. *Free Radical Biol. Med. 49*, 2040−2048.
(54) Ahmad, N., Misra, M., Husain, M. M., and Srivastava, R. C. (1996) Metal-independent putative superoxide dismutase mimics in chemistry, biology, and medicine. *Ecotoxicol. Environ. Saf. 34*, 141−144.
(55) Kim, H. J., Graham, D. W., DiSpirito, A. A., Alterman, M. A., Galeva, N., Larive, C. K., Asunskis, D., and Sherwood, P. M. (2004) Methanobactin, a copper-acquisition compound from methane-oxidizing bacteria. *Science 305*, 1612−1615.
(56) Choi, D. W., Semrau, J. D., Antholine, W. E., Hartsel, S. C., Anderson, R. C., Carey, J. N., Dreis, A. M., Kenseth, E. M., Renstrom, J. M., Scardino, L. L., Van Gorden, G. S., Volkert, A. A., Wingad, A. D., Yanzer, P. J., McEllistrem, M. T., de la Mora, A. M., and DiSpirito, A. A. (2008) Oxidase, superoxide dismutase, and hydrogen peroxide reductase activities of methanobactin from types I and II methanotrophs. *J. Inorg. Biochem. 102*, 1571−1580.
(57) Kenney, G. E., and Rosenzweig, A. C. (2012) Chemistry and biology of the copper chelator methanobactin. *ACS Chem. Biol. 7*, 260−268.
(58) Graham, D. W., and Kim, H. J. (2011) Production, isolation, purification, and functional characterization of methanobactins. *Methods Enzymol. 495*, 227−245.
(59) Mulvey, M. A., Schilling, J. D., and Hultgren, S. J. (2001) Establishment of a persistent Escherichia coli reservoir during the acute phase of a bladder infection. *Infect. Immun. 69*, 4572−4579.
(60) Datsenko, K. A., and Wanner, B. L. (2000) One-step inactivation of chromosomal genes in Escherichia coli K-12 using PCR products. *Proc. Natl. Acad. Sci. U.S.A. 97*, 6640−6645.
(61) Murphy, K. C., and Campellone, K. G. (2003) Lambda Red-mediated recombinogenic engineering of enterohemorrhagic and enteropathogenic E. coli. *BMC Mol. Biol. 4*, 11.
(62) Freter, R., Allweiss, B., O'Brien, P. C., Halstead, S. A., and Macsai, M. S. (1981) Role of chemotaxis in the association of motile bacteria with intestinal mucosa: in vitro studies. *Infect. Immun. 34*, 241−249.
(63) Hancock, J. T., and Jones, O. T. (1987) The inhibition by diphenyleneiodonium and its analogues of superoxide generation by macrophages. *Biochem. J. 242*, 103−107.
(64) Acevedo, O., and Jorgensen, W. L. (2010) Advances in quantum and molecular mechanical (QM/MM) simulations for organic and enzymatic reactions. *Acc. Chem. Res. 43*, 142−151.
(65) Ohlinger, W. S., Klunziger, P. E., Deppmeier, B. J., and Hehre, W. J. (2009) Efficient calculation of heats of formation. *J. Phys. Chem. A 113*, 2165−2175.
(66) Fromager, E. (2011) Rigorous formulation of two-parameter double-hybrid density-functionals. *J. Chem. Phys. 135*, 244106.
(67) Zawada, A., Kaczmarek-Kedziera, A., and Bartkowiak, W. (2012) On the potential application of DFT methods in predicting the interaction-induced electric properties of molecular complexes. Molecular H-bonded chains as a case of study. *J. Mol. Model. 18*, 3073−3086.
(68) Morschel, P., Janikowski, J., Hilt, G., and Frenking, G. (2008) Ligand-tuned regioselectivity of a cobalt-catalyzed Diels-Alder reaction. A theoretical study. *J. Am. Chem. Soc. 130*, 8952−8966.
(69) Bailey, W. C. (1998) B3LYP calculation of deuterium quadrupole coupling constants in molecules. *J. Mol. Spectrosc. 190*, 318−323.
(70) Rydberg, P., and Olsen, L. (2009) The accuracy of geometries for iron porphyrin complexes from density functional theory. *J. Phys. Chem. A 113*, 11949−11953.
(71) Ansbacher, T., Srivastava, H. K., Martin, J. M., and Shurki, A. (2010) Can DFT methods correctly and efficiently predict the coordination number of copper(I) complexes? A case study. *J. Comput. Chem. 31*, 75−83.
(72) Scott A.P., R. L. (1996) Harmonic vibrational frequencies: An evaluation of Hartree-Fock, Moller-Plesset, quadratic configuration interaction, density functional theory, and semiempirical scale factors. *J. Phys. Chem. 100*, 16502−16513.
(73) Shephard, M. J., and Paddon-Row, M. N. (1995) Gas phase structure of the bicyclo [2.2.1] heptane (Norbornane) cation radical: A combined ab initio MO and density functional theory. *J. Phys. Chem. 99*, 3101−3108.
(74) Turecek, F. (1998) Proton affinity of dimethyl sulfoxide and relative stabilities of C_2H_6OS molecules and C_2H_7OS+ ions. A comparative G2(MP2) ab initio and density functional theory study. *J. Phys. Chem.*, 102.